Analysis of static var compensator-based distance protection of transmission network considering different line lengths: a case study of nigerian grid

Akintunde Samson Alayande (alayandeakintundesamson@gmail.com)
Department of Electrical Engineering and Centre for Energy & Electric Power, Tshwane University of Technology, Pretoria, Gauteng, South Africa

Olawale Popoola
Department of Electrical Engineering and Centre for Energy & Electric Power, Tshwane University of Technology, Pretoria, Gauteng, South Africa

Sunday Oluwagbenga Akinbode
Department of Electrical and Electronics Engineering, Faculty of Engineering, University of Lagos, Lagos, Nigeria

Research Article

Keywords: Static Var Compensators, Distance relay protection, Error margins, Flexible Alternating Current Transmission Systems, Voltage profile

Posted Date: May 18th, 2022

DOI: https://doi.org/10.21203/rs.3.rs-1667545/v1

Abstract

This paper presents a Matlab/Simulink-based approach for investigating the performance of Static Var Compensators (SVCs) on distance relay protection installed at varying lengths of the practical Nigerian 132-kV sub-transmission grid system. The shunt-connected SVC is located at the Ikorodu sub-station end of the Ikorodu-Sagamu 132-kV transmission line. The faults are simulated on a short line (18.4 km), medium line (100 km) and long line (226 km) in the Matlab/Simulink model of the Ikorodu-sagamu 132kV sub-transmission distance protection scheme. The results obtained are then used to investigate the impact SVCs have on distance protection relays when they are connected and disconnected for varying transmission line lengths whilst keeping all other parameters constant. The results obtained show that the SVC despite being advantageous, also introduces under-reach and over-reach tendencies for different zone faults (zones 1 and 2) as simulated on varying lengths of 132-kV transmission lines. This implies that a further simulation is required to recommend measures aimed at reducing the error margin introduced by the SVCs.

Introduction

Flexible Alternating Current Transmission Systems (FACTS) devices such as SVCs are one of the most versatile which help to regulate reactive power and improve system voltage [1]. Universally, SVCs are being sought after in the mining, power, energy, railway industries to mitigate losses and foster plant efficiency [2]. In Nigeria, the Transmission Company of Nigeria (TCN) has embraced the idea of employing FACTS devices for efficient dispatch of quality power to its customers [3]. The distance protective relays are electrical devices which make use of electrical quantities (voltage and current) in order to calculate and compare the apparent fault impedance with a pre-calculated value of zone protections. The protective relay has four zones of protection namely zone 1, zone 2, zone 3 and zone 3 reverse. Zone 1 covers 80–90% of the protected line, zone 2 covers 100% of the protected line plus 20–50% of the next adjacent line, zone 3 covers 100% of the protected line plus 125% of the next adjacent line and zone 3 reverse covers 10–20% of the protected line in the reverse direction. Adequate current and time grading of all protective relays is paramount to prevent nuisance tripping [4].

The distance protective relays can be installed on any length of transmission line network such as short line (transmission line less than 50km), medium line (lines are more than 50km but less than 150km) or long line (transmission line having lengths greater than 150km) [5]. Although, SVCs improve the overall system efficiency and reduce transmission line losses, the introduction of SVCs on varying lengths of transmission lines in this research resulted in the under or over reach characteristics of the protective relay.

.

Theoretical Framework And Mathematical Formulations

Transmission lines are prone to shunt faults. These faults are mostly highly resistive in nature. The various categories of transmission line will help us study the effect SVCs will have on distance protective relays when they are installed on varying lengths of transmission lines.

Short transmission line model

Short length transmission lines are predominantly classified as lines whose length are less than 50km [5]. Owing to their short length, only the resistance and inductance are considered, the capacitance effects are small and disregarded. Figure 1 shows the equivalent circuit of a short transmission line. The short transmission line can be mathematically modelled as shown below;

$$V_S = Sendingendvoltageperphase$$

$$V_R = Receivingendvoltageperphase$$

$$I_S = Sendingendcurrentperphase$$

$$I_R = Loadcurrentperphase$$

$$R = Resistanceperphase$$

$$X_L = Inductivereactanceperphase$$

$$C = Capacitanceperphase$$

$$Cos_{\emptyset_R} = Receivingendpowerfactor(Lagging)$$

$$Sin_{\emptyset_R} = Sendingendpowerfactor(Lagging)$$

$$V_S = V_R + IRCos_{\emptyset_R} + IX_L Sin_{\emptyset_R}$$

1

$$* V_R = V_R + j0$$

2

where

$$\vec{I} = \vec{I}\angle - \emptyset_R = I(Cos\emptyset_R - Sin\emptyset_R)$$

\stackrel{^}{Z}=R+j{X}_{L}

3

\stackrel{^}{{V}_{S}}= \stackrel{^}{{V}_{R}}+\stackrel{^}{I}\stackrel{^}{Z}

4

\overrightarrow{{V}_{S}}= {V}_{R}+j0+I\left(Cos{\varnothing }_{R}-Sin{\varnothing }_{R}\right)(R+j{X}_{L})

5
\overrightarrow{{V}_{S}}= {V}_{R}+\left(IRCos{\varnothing }_{R}+I {X}_{L}Sin{\varnothing }_{R}\right)+j\left(I {X}_{L}Cos{\varnothing }_{R}-IRSin{\varnothing }_{R}\right)
6
\overrightarrow{{V}_{S}}= \sqrt{{\left({V}_{R}+IRCos{\varnothing }_{R}+I{X}_{L}Sin{\varnothing }_{R}\right)}^{2}+{\left(I{X}_{L}Cos{\varnothing }_{R}-IRSin{\varnothing }_{R}\right)}^{2} }
7
\therefore {V}_{S}= {V}_{R}+IR {Cos}_{{\varnothing }_{R}}+I{X}_{L}{Sin}_{{\varnothing }_{R}}
8

Medium transmission line model

Medium length transmission lines are typically categorized as lines whose length are between 50km and 150km [5]. The capacitance to ground effect is considered here as it has an effect on the transmission line. The capacitance of the line is usually uniformly distributed but for ease of calculation, the three methods that are usually explored are as described in the subsections that follows :

2.2.1 End condenser model

This method considers the capacitance of the line to be lumped at the receiving end of the line. This is the simplest method but its drawback lies in the over estimation of the line capacitance and computational errors due to the assumption that all the capacitance is at the receiving end of the line are up to 10% [5]. Figure 2 shows the equivalent circuit for the end condenser modelling of a medium transmission line. The end condenser method can be mathematically modelled to resolve the medium transmission line as presented below.

\stackrel{˙}{{V}_{R}}= {V}_{R}+j0
9
\stackrel{˙}{{I}_{S}}= \stackrel{˙}{{I}_{R}}+\stackrel{˙}{{I}_{C}}
10
\overrightarrow{{I}_{R}}= {I}_{R}\left(\text{cos}{\varnothing }_{R}-j\text{sin}{\varnothing }_{R}\right)
11
\stackrel{˙}{{I}_{C}}=j\stackrel{˙}{{V}_{R}}?C=j2pfC\stackrel{˙}{{V}_{R}}
12
\overrightarrow{{I}_{S}}= {I}_{R}\left(\text{cos}{\varnothing }_{R}-j\text{sin}{\varnothing }_{R}\right)+ j2\pi fC{V}_{R}
13
\overrightarrow{{I}_{S}}= {I}_{R}\text{cos}{\varnothing }_{R}+j\left(-{I}_{R}\text{sin}{\varnothing }_{R}+2\pi fC{V}_{R}\right)
14
\stackrel{˙}{{I}_{S}}= \stackrel{˙}{{I}_{S}}\stackrel{˙}{Z}

15
$$\stackrel{`}{{I}_{S}}= \stackrel{`}{{I}_{S}}\left(R+j{X}_{L}\right)$$
16
$$\stackrel{`}{{V}_{S}}= \stackrel{`}{{V}_{R}}+\stackrel{`}{{I}_{S}}\stackrel{`}{Z}$$
17
$$\stackrel{`}{{V}_{S}}= \stackrel{`}{{V}_{R}}+\stackrel{`}{{I}_{S}}\left(R+j{X}_{L}\right)$$
18

Nominal-T model

This method considers the capacitance of the line to be concentrated at the midpoint of the line[5]. This implies that half of the line resistance and inductance are lumped on either sides. Figure 3 shows the Nominal T method of modelling a medium length transmission line. The Nominal T method can be mathematically modelled to resolve the medium transmission line as shown below;

$$\stackrel{`}{{V}_{R}}= {V}_{R}+j0$$
19
$$\overrightarrow{{I}_{R}}= {I}_{R}\left(\text{cos}{\varnothing }_{R}-j\text{sin}{\varnothing }_{R}\right)$$
20

Voltage across Capacitor C is given as;

$$\stackrel{`}{{V}_{1}}= \stackrel{`}{{V}_{R}}+ \stackrel{`}{{I}_{R}} \stackrel{`}{Z}/2$$
21
$$\overrightarrow{{V}_{1}}= {V}_{R}+ {I}_{R}\left(\text{cos}{\varnothing }_{R}-j\text{sin}{\varnothing }_{R}\right)\left(\frac{R}{2}+j\frac{{X}_{L}}{2}\right)$$
22
$$\overrightarrow{{I}_{C}}=j\omega C{V}_{1}=j2\pi fC{V}_{1}$$
23
$$\stackrel{`}{{I}_{S}}= \stackrel{`}{{I}_{R}}+\stackrel{`}{{I}_{C}}$$
24
$$\stackrel{`}{{V}_{S}}= \stackrel{`}{{V}_{1}}+\stackrel{`}{{I}_{S}} \stackrel{`}{\frac{Z}{2}}$$
25
$$\stackrel{`}{{V}_{S}}= \stackrel{`}{{V}_{1}}+\stackrel{`}{{I}_{S}} \left(\frac{R}{2}+j\frac{{X}_{L}}{2}\right)$$
26

2.2.2 Nominal-pi model

This method considers the capacitance of the line to be divided into two halves and lumped both at the receiving end and at the sending end [5]. The capacitance at the sending end does not have any significance with line drop. However, the line charging current must be considered when calculating for the total sending end current. Figure 4 shows the equivalent circuit for a Nominal modelling of a

medium length transmission line. The Nominal π Method can be mathematically modelled to resolve the medium transmission line as shown below;

\stackrel{`}{{V}_{R}}= {V}_{R}+j0
27
\overrightarrow{{I}_{R}}= {I}_{R}\left(\text{cos}{\varnothing }_{R}-j\text{sin}{\varnothing }_{R}\right)
28
\stackrel{`}{{I}_{C1}}=j?\left(\frac{C}{2}\right)\stackrel{`}{{V}_{R}}=jpfC\stackrel{`}{{V}_{R}}
29
\stackrel{`}{{I}_{L}}= \stackrel{`}{{I}_{R}}+\stackrel{`}{{I}_{C1}}
30
\stackrel{`}{{V}_{S}}= \stackrel{`}{{V}_{R}}+\stackrel{`}{{I}_{L}}\stackrel{`}{Z}
31
\stackrel{`}{{V}_{S}}= \stackrel{`}{{V}_{R}}+\stackrel{`}{{I}_{L}}\left(R+j{X}_{L}\right)
32
\stackrel{`}{{I}_{C2}}=j?\left(\frac{C}{2}\right)\stackrel{`}{{V}_{S}}=jpfC\stackrel{`}{{V}_{S}}
33
\stackrel{`}{{I}_{S}}= \stackrel{`}{{I}_{L}}+\stackrel{`}{{I}_{C2}}
34

2.3 Long Transmission Line

Long transmission lines are typically categorized as lines in which their length is greater than 150km [5]. The effect of all parameters are considered and as such the calculations are rigorous. The resistance and inductive reactance are both series elements while the leakage susceptance and leakage conductance are shunt elements [5]. Figure 5 shows the equivalent circuit of a Long transmission line. The long transmission line can be mathematically modelled as shown below;

z=Series impedancemof the line per phase
y=shunt admittance of the line per phase
v=Voltage at the end of the element towards the receiving end
v+dv=Voltage at the end of the element towards the sending end
I+dI=Current entering the element dx
I=current leaving the element dx

For the small element dx;

z dx=series impedance
35
y dx=shunt admittance
36
dV=Iz dx

37
\frac{dV}{dx}=Iz
38
dI=current through shunt admittance of element
\frac{dV}{dx}=V y
39

By differentiating with respect to x

\frac{{d}^{2}V}{{dx}^{2}}=z \frac{dI}{dx}=z \left(V y\right)
40
? \frac{dI}{dx}=V.y
41
\frac{{d}^{2}V}{{dx}^{2}}=y z V
42

Solving the differential equation gives;

V= {k}_{1}\text{cosh}\left(x\sqrt{yz}\right)+{k}_{2}\text{sinh}\left(x\sqrt{yz}\right)
43

Differentiating with respect to x;

\frac{dV}{dx}={k}_{1}\sqrt{yz}\text{sinh}\left(x\sqrt{yz}\right)+
{k}_{2}\sqrt{yz}\text{cosh}\left(x\sqrt{yz}\right)
44
\frac{dV}{dx}=I z
45
Iz= {k}_{1}\sqrt{yz}\text{sinh}\left(x\sqrt{yz}\right)+ {k}_{2}\sqrt{yz}\text{cosh}\left(x\sqrt{yz}\right)
46
I= \sqrt{\frac{y}{z}}\left[{k}_{1}\text{sinh}\left(x\sqrt{yz}\right)+
{k}_{2}\text{cosh}\left(x\sqrt{yz}\right)\right]
47

Getting the values for constant k_1 and k_2

At X=0, V= {V}_{R }andI= {I}_{R}

Inserting the above values into Eq. 43

V= {k}_{1}\text{cosh}\left(0\right)+{k}_{2}\text{sinh}\left(0\right)
V= {k}_{1}+ 0
V= {k}_{1}

At X=0, V= {V}_{R }andI= {I}_{R}

Inserting the above values into Eq. (47) results to

{I}_{R}= \sqrt{\frac{y}{z}}\left[{k}_{1}\text{sinh}\left(0\right)+ {k}_{2}\text{cosh}\left(0\right)\right]
{k}_{2}= \sqrt{\frac{z}{y}} {I}_{R}
48

Substituting values of k_1 and k_2 into Eq. 43

V= {k}_{1}\text{cosh}\left(x\sqrt{yz}\right)+{k}_{2}\text{sinh}\left(x\sqrt{yz}\right)
V= V\text{cosh}\left(x\sqrt{yz}\right)+\sqrt{\frac{z}{y}} {I}_{R}\text{sinh}\left(x\sqrt{yz}\right)
I= \sqrt{\frac{y}{z}}\left[V\text{sinh}\left(x\sqrt{yz}\right)+\sqrt{\frac{z}{y}} {I}_{R}
\text{cosh}\left(x\sqrt{yz}\right)\right]
49

Therefore, the sending end voltage (V_S) and sending end current (I_S) can be obtained by equating x = l in equations (43) and (47) as

{V}_{S}= {V}_{R}\text{cosh}\left(l\sqrt{yz}\right)+ \sqrt{\frac{z}{y}}{I}_{R}\text{sinh}\left(l\sqrt{yz}\right)
50
{I}_{S}=\sqrt{\frac{y}{z}}{V}_{R}\text{sinh}\left(l\sqrt{yz}\right)+ {I}_{R}\text{cosh}\left(l\sqrt{yz}\right)
51

with

l\sqrt{yz}= \sqrt{l y . l z}= \sqrt{YZ}
51
\sqrt{\frac{y}{z}}=\sqrt{\frac{y l}{z l}}= \sqrt{\frac{Y}{Z}}
52

where

Y=total shunt admittance of thr line
Z=total series admittance of thr line

Therefore, we can express VS and IS as;

{V}_{S}= {V}_{R}\text{cosh}\left(\sqrt{YZ}\right)+ \sqrt{\frac{Z}{Y}}{I}_{R}\text{sinh}\left(\sqrt{YZ}\right)
53
{I}_{S}=\sqrt{\frac{Y}{Z}}{V}_{R}\text{sinh}\left(\sqrt{YZ}\right)+ {I}_{R}\text{cosh}\left(\sqrt{YZ}\right)
54

3.1. *Concept of distance protection*

Protection of transmission lines is paramount but also more important is the accuracy of determining the exact fault location. Figure 6 shows the illustration of a distance relay positioned at point A who has a reach of Z_{set}. The relay is designed to respond to faults within its zone of protection. The distance relay can be divided into three major zones of protection namely zone 1, zone 2 and zone 3.

3.2 Choice between impedance, reactance and mho algorithm

Various architectures are available for use on distance protective relays. Impedance relays are known to be affected by arc resistance faults, thus their low patronage. Reactance relays are known to be effective against ground faults for short lines rather than long lines. The mho relay is considered for use in this research as it is more widely accepted due to it being less affected by arc resistance faults [6].

Results And Discussion

MATLAB/SIMULINK model

The single line diagram of the transmission line network used as a case study is as shown in Fig. 7. A brief description of each of the components modelled in the MATLAB/ SIMULINK environment is presented in the sub section that follows.

4.1 *The distance relay Simulink model*

The distance relay is simulated in the Matlab/Simulink environment by the interaction of various math operators, current signals, voltage signals and logic operators.

The impedance as measured by the distance protective relay in the event of a fault is compared to the calculated line impedance setting of the transmission line. The zone which the fault belongs to is identified and the fault the distance rellocation calculated accordingly by the logic. The distance relay then sends out a trip signal to the circuit breaker in order to isolate the circuit breaker from the network [7].

The distance relay model comprises of the tripping signal block, time delay block, zone detection block, impedance measurement block, fault identification & detection block [7]. The distance relay and SVC are incorporated with the simulated transmission line model as shown in Fig. 6. The SVC considered in this research was originally designed by Pierre Giroux and Gilbert Sybille (Hydro-Quebec) and accepted into (MATHWORKS) MATLAB repository. The SVC model comprises of 3 nos Thyristor switched Capacitor (TSC) of 94MVAR each and 1 no Thyristor controlled reactor (TCR) 109MVAR. Pierre & Gilbert originally designed the SVC to operate on a 735kV 60Hz transmission line coupled with 200MW load but the SVC model Voltage and frequency parameters was adjusted to match our input voltage of 132kV and 50Hz respectively while all other parameters remained the same as the original model designed [8].

4.2 *The mho circle characteristics Simulink model*

The Mho characteristics depicted in Fig. 8 outlines the relationship between reactance and resistance on a transmission line. This is used to explain the operation of the relay in this subheadings that follows.

4.4 The Static Var Compensator (SVC) Simulink and control model

The distance relay model explored is as shown in Fig. 9 comprises of the fault locator, mho circle characteristics graph, impedance measurement black, zone detection block, fault detection and identification block.

The SVC model incorporated into this research work is shown below in Fig. 10. It was designed by Pierre Giroux and Gibert Sybille (Hydro-Quebec). SVCs are shunt-connected devices responsible for voltage profile correction and reduction of transmission line losses. The model designed by the authors was used to investigate the effect of harmonics, transients and stresses on power components during fault situations. The model's voltage and frequency parameters were revised in order to align with the requirements of this research.

Table 1 outlines the results obtained when the SVC is connected and disconnected from a short transmission line of 18.4km for both faults in zone 1 and zone 2. The analysis in Table 1 was based on the simulation of five different types of faults on the power grid network considering zone 1 and zone 2. For example, in zone 1, considering a Single Line-to-Earth fault, the Resistance-Reactance (R-X) diagram for the distance relay when SVC is connected with the transmission line is shown in Fig. 11 (a) while Fig. 11 (b) shows the Resistance-Reactance (R-X) diagram for the distance relay when SVC is not connected for the same L-E type of fault. Figure 11a and Fig. 11b clearly show plotted points at different magnitudes of Resistance and Reactance as shown in Table 1 for both Line-to-Earth faults with and without the SVC connected to the bus. Consequently, with SVC connected and SVC disconnected the distance relay was observed to have tripped at 11.49 km and 8.311 km respectively. Thus, indicating that during single-line-to-earth fault conditions, the distance relay over-reaches with the SVC connected.

The controlled firing of the thyristors in order to coordinate the addition or reduction of VAR in the system is done by the SVC control system. The SVC Control system comprises of four modules which includes the distribution unit, measurement system, firing unit, and voltage regulator [8]–[10]. The simulations were carried out considering faults occurring in zone 1 and zone 2 of the distance protective relay.

Table 1
Simulation result for the impedance and fault location for a 18.4km short line as seen by the distance relay modelled in MATLAB/Simulink

Protection zone	SVC connection status		Type of faults				
			L-E fault	L-L fault	L-L-L fault	L-L-E fault	L-L-L-E fault
zone 1	with svc	apparent impedance	0.7067 + j1.594	0.7067 + j1.594	0.7067 + j1.594	1.006 + j1.992	0.7067 + j1.594
		fault location	11.49 km	11.49 km	11.49 km	14.70 km	11.49 km
zone 1	without svc	apparent impedance	0.4075 + j1.194	0.7067 + j1.594	0.7067 + j1.594	1.006 + j1.992	0.7067 + j1.594
		fault location	8.311 km	11.49 km	11.49 km	14.70 km	11.49 km
summary for zone 1 distance relay			Over reach	Same	Same	Same	Same
zone 2	with svc	apparent impedance	2.482 + j5.539	2.472 + j5.029	2.472 + j5.029	2.482 + j5.042	2.482 + j5.042
		fault location	39.99 km	36.92 km	36.92 km	37.03 km	37.03 km
zone 2	without svc	apparent impedance	2.482 + j5.539	2.473 + j5.029	2.473 + j5.029	2.482 + j5.042	2.482 + j5.042
		fault location	39.99 km	36.92 km	36.92 km	37.03 km	37.03 km
summary for zone 2 distance relay			Same	Same	Same	Same	Same

When the simulation was carried out for other types of shunt faults such as Double-Line-to-Earth fault, Phase-to-Phase faults, Three-Phase-to-Earth faults, the Resistance -Reactance (R-X) diagram for the distance relay when SVC is connected and not connected remains the same. Table 1 shows the results for Double-Line-to-Earth fault, Phase-to-Phase faults, Three-Phase-to-Earth faults with and without the SVC connected to the bus. The results presented shows that the distance relay tripped at 11.49 km. The implication of this is that during these faults conditions with SVC connected or not connected, the distance relay fault location accuracy is not affected.

Similarly, for zone 2, when the simulation was carried out for all types of shunt faults such as single Line to earth fault, Double-Line-to-Earth fault, Phase-to-Phase faults, Three-Phase-to-Earth faults, the Resistance-Reactance (R-X) diagram for the distance relay when SVC is connected and not connected remains the same as shown in Fig. 12. Table 1 shows the results for single Line to earth fault, Double-Line-to-Earth fault, Phase-to-Phase faults, Three-Phase-to-Earth faults with and without the SVC

connected to the bus. Consequently, for all the shunts mentioned above, the distance relay was observed to have tripped at 39.99 km, 37.03 km, 36.92 km and 37.03 for their respective fault types. Thus, indicating that during single Line to earth fault, Double-Line-to-Earth fault, Phase-to-Phase faults, Three-Phase-to-Earth faults conditions with SVC connected or not connected, the distance relay fault location accuracy is not affected.

Table 2 outlines the results obtained when the SVC is connected and disconnected from a medium length transmission line of 100km for both faults in zone 1 and zone 2. The analysis in Table 2 was based on the simulation of five different types of faults on the power grid network considering zone 1 and zone 2. For example, in zone 1, considering the Three-Phase-to-Earth fault and Three-Phase faults, the Resistance-Reactance (R-X) diagram for the distance relay when SVC is connected with the transmission line is shown in Fig. 13 (a) while Fig. 13 (b) shows the Resistance-Reactance (R-X) diagram for the distance relay when SVC is not connected for the same Three-Phase-to-Earth fault. Figure 13a and Fig. 13b clearly shows plotted points at different magnitudes of Resistance and Reactance as shown in Table 2 for both Three-Phase-to-Earth fault and Three-Phase faults with and without the SVC connected to the bus. Therefore, with SVC connected and SVC disconnected the distance relay was observed to have tripped at 73.52 km and 80.00 km respectively. Thus, indicating that the distance relay under-reaches with the SVC connected for Three-Phase-to-Earth fault and Three-Phase faults.

When the simulation was carried out for other types of shunt faults such as Single-Line-to-Earth fault, Double-Line-to-Earth fault and Phase-to-Phase faults the Resistance-Reactance (R-X) diagram for the distance relay when SVC is connected and not connected remains the same. Table 2 shows the results for Single-Line-to-Earth fault, Double-Line-to-Earth fault and Phase-to-Phase faults with and without the SVC connected to the bus. Consequently, for all the shunt faults mentioned above, the distance relay was observed to have tripped at approximately 80.00 km. Thus, indicating that during Single-Line-to-Earth fault, Double-Line-to-Earth fault and Phase-to-Phase faults conditions with SVC connected or not connected, the distance relay fault location accuracy is not affected.

Table 2
Simulation result for the impedance and fault location for a 100km medium line as seen by the distance relay modelled in MATLAB/Simulink

Protection zone	SVC connection status		Type of faults				
			L-E fault	L-L fault	L-L-L fault	L-L-E fault	L-L-L-E fault
zone 1	with svc	apparent impedance	5.467 + j10.840	5.467 + j10.820	4.869 + j10.040	5.467 + j10.820	4.869 + j10.040
		fault location	80.00 km	79.85 km	73.52 km	79.87 km	73.52 km
zone 1	without svc	apparent impedance	5.467 + j10.840	5.467 + j10.840	5.467 + j10.840	5.467 + j10.840	5.467 + j10.840
		fault location	79.97 km	79.97 km	80.00 km	79.98 km	80.00 km
summary for zone 1 distance relay			Same	Same	under reach	Same	under reach
zone 2	with svc	apparent impedance	2.858 + j9.139	2.858 + j9.139	2.858 + j9.139	2.229 + j30.37	2.858 + j9.139
		fault location	63.09 km	63.09 km	63.09 km	200.6 km	63.09 km
zone 2	without svc	apparent impedance	4.466 + j21.41	4.466 + j21.41	4.466 + j21.41	4.466 + j21.41	4.466 + j21.41
		fault location	144.1 km	144.1 km	144.1 km	144.1 km	144.1 km
summary for zone 2 distance relay			under-reach	under-reach	under-reach	over-reach	under-reach

Considering zone 2, for Single Line-to-Earth fault, Phase-to-Phase faults and three-Phase-to-Earth faults, the Resistance-Reactance (R-X) diagram for the distance relay when SVC is connected with the transmission line is shown in Fig. 14 (a) while Fig. 14 (b) shows the Resistance-Reactance (R-X) diagram for the distance relay when SVC is not connected for the same fault types mentioned above. Figure 14a and Fig. 14b clearly shows plotted points at different magnitudes of Resistance (R) and Reactance (X) for when the SVC is connected and disconnected. Subsequently, the distance relay, with SVC connected and disconnected was observed to have tripped at 63.09 km and 144.1 km respectively. Thus, indicating that the distance relay under-reaches with the SVC connected for Single Line-to-Earth fault, Phase-to-Phase faults and three-Phase-to-Earth faults.

Similarly, for zone 2, when the simulation was carried out for Double-Line-to-Earth fault, the Resistance-Reactance (R-X) diagram for the distance relay when SVC is connected and not connected are observed

to be different. Table 2 shows the results for a Double-Line-to-Earth fault with and without the SVC connected to the bus. Therefore, for a Double-Line-to-Earth fault with SVC connected and disconnected, the distance relay was observed to have tripped at 200.6 km, and 144.1 km respectively. Therefore, the distance relay over reaches with the SVC connected for Double-Line-to-Earth faults.

Table 3 outlines the results obtained when the SVC is connected and disconnected from a long transmission line of 226 km for both faults in zone 1 and zone 2. The analysis in Table 3 was based on the simulation of five different types of faults on the power grid network considering zone 1 and zone 2. For example, in zone 1, considering the Line-to-Earth fault, the Resistance-Reactance (R-X) diagram for the distance relay when SVC is connected with the transmission line is shown in Fig. 15 (a) while Fig. 15 (b) shows the Resistance-Reactance (R-X) diagram for the distance relay when SVC is not connected for the same Line-to-Earth fault. Figure 15a and Fig. 15b clearly shows plotted points at different magnitudes of Resistance and Reactance as shown in Table 3 for all types of shunt faults with and without the SVC connected to the bus. Therefore, with SVC connected and SVC disconnected the distance relay was observed to have tripped at 174.30 km and 180.80 km respectively. Thus, indicating that the distance relay under-reaches with the SVC connected for Line-to-Earth faults.

When the simulation is carried out for other types shunt faults such as Double-Line-to-Earth fault, Three-Phase-to-Earth fault and Phase-to-Phase faults, the Resistance-Reactance (R-X) diagram for the distance relay when SVC is connected and not connected under reaches for all shunt fault types mentioned above. Table 3 shows the results for Double-Line-to-Earth fault, Three-Phase-to-Earth fault and Phase-to-Phase faults with and without the SVC connected to the bus. Consequently, for all the shunts mentioned above, the distance relay was observed to have tripped at approximately 182.60 km, 181.90 km and 182.60 km respectively. Thus, indicating that during Double-Line-to-Earth fault, Three-Phase-to-Earth fault and Phase-to-Phase fault conditions with SVC connected or not connected, the distance relay fault location accuracy is affected.

Considering zone 2, for Double-Line-to-Earth faults, the Resistance-Reactance (R-X) diagram for the distance relay when SVC is connected with the transmission line is shown in Fig. 16 (a) while Fig. 16 (b) shows the Resistance-Reactance (R-X) diagram for the distance relay when SVC is not connected. Figure 16a and Fig. 16b clearly shows plotted points at the different magnitude of Resistance (R) and Reactance (X) for when the SVC is connected and disconnected. Subsequently, the distance relay, with SVC-connected and disconnected was observed to have tripped at 250.40 km and 248.40 km respectively. Thus, indicating that the distance relay over-reaches with the SVC connected for Double-Line-to-Earth faults.

Similarly, for zone 2, when the simulation is carried out for Line-to-Earth faults, Three-Phase-tot-Earth fault, Phase-to-Phase faults, the Resistance-Reactance (R-X) diagram for the distance relay when SVC is connected and not connected are observed to be different. Table 3 shows the results for Double-Line-to-Earth fault with and without the SVC connected to the bus. Therefore, for Line-to-Earth faults, Three-Phase-tot-Earth fault, Phase-to-Phase faults, with SVC connected and disconnected, the distance relay

was observed to have tripped at 250.40km and 235.50km, 250.40km and 247.80km, 250.40km and 247.80km respectively. Therefore, the distance relay over reaches with the SVC connected for all shunt type of faults as earlier mentioned.

Table 3
Simulation result for the impedance and fault location for a 226 km long line as seen by the distance relay modelled in MATLAB/Simulink

Protection zone	SVC connection status		Type of faults				
			L-E fault	L-L fault	L-L-L fault	L-L-E fault	L-L-L-E fault
zone 1	with svc	apparent impedance	11.76 + j23.70	11.76 + j23.70	11.76 + j23.70	11.76 + j23.70	11.76 + j23.70
		fault location	174.30 km	174.30 km	174.30 km	174.30 km	174.30 km
zone 1	without svc	apparent impedance	12.36 + j24.50	12.00 + j24.98	12.36 + j24.50	12.00 + j24.98	12.12 + j24.81
		fault location	180.80 km	182.60 km	180.80 km	182.60 km	181.90 km
summary for zone 1 distance relay			under-reach	under-reach	under-reach	under-reach	under-reach
zone 2	with svc	apparent impedance	16.10 + j34.43	16.10 + j34.43	16.10 + j34.43	16.10 + j34.43	16.10 + j34.43
		fault location	250.40 km	250.40 km	250.40 km	250.40 km	250.40 km
zone 2	without svc	apparent impedance	13.12 + j33.27	16.49 + j33.91	16.62 + j33.73	16.49 + j33.91	16.63 + j33.73
		fault location	235.50 km	248.40 km	247.80 km	248.40 km	247.80 km
summary for zone 2 distance relay			over-reach	over-reach	over-reach	over-reach	over-reach

4.6 Summary of results

The simulation result when a highly inductive load of 130MVAR is applied into the real-life scenario setting of Ikorodu-Sagamu 132kV transmission line settings being fed from a source of 600MVA short circuit is analyzed. The simulation result shows a case of very high voltage despite the highly inductive load due to the surplus amount of source power.

From the simulation results observed and documented for zone 1 and zone 2 in Table 1, Table 2, Table 3, Fig. 17(a), Fig. 17(b) and Fig. 17(c) the following observations were made when the known fault application points are varied directly with the short, medium and long lines considered in the simulation.

1. For short lines, when the SVC is applied, the simulation shows us that for both zone 1 and zone 2 faults, the SVC has little or no impact on the fault location as only single line to earth fault in zone 1 (10% of the total faults simulated) showed that the distance relay under reached when the SVC was connected. All other shunt type fault simulation carried out on the distance relay showed no cases of under reach or over reach.
2. For medium lines, when the SVC is applied, the simulation shows us that for both zone 1 and zone 2 faults, the SVC has a large impact on the fault location as all the shunt type of faults with the exception of single line to earth fault in zone 1, phase to phase fault in zone 1 and double line to earth fault in zone 1 (30% of the total faults simulated) showed that the distance relay under reached when the SVC was connected. The double line to earth fault in zone 2 was observed to have over reached when the SVC was connected.
3. For long lines, when the SVC is applied, the simulation shows us that for both zone 1 and zone 2 faults, the SVC has a large impact on the fault location as all the shunt type of faults under-reached for faults in zone 1 (100% of the total faults simulated). Thus, the distance relay under reached when the SVC was connected. In addition, for all shunt type of faults simulated in zone 2, the distance protection relays were observed to have over-reached for fault types when the SVC was connected.

Furthermore, the distance protective relays see these fault locations as either over-reach or under-reach. The over-reach and under-reach are evidence that error margins are introduced when SVCs are connected. Similarly, Fig. 17(a), Fig. 17(b) and Fig. 17(c) shows Bar charts for short, medium and long transmission lines respectively for the easy comparison for each fault type with and without SVC connected.

SVCs appear to have increasing effect on distance protective relays as the length of the transmission line is increased. The under-reach characteristics of the distance relay tends to be more consistent with the increase in the length of the transmission line. Figure 17(a), Fig. 17(b) and Fig. 17(c) shows graphically the under reach and over reach tendencies of the distance protective relays.

Conclusion

The optimization of transmission line is very crucial.

The use of SVCs is gaining ground due to its low cost compared to other FACTS devices.

In this research, the result gotten and scrutinized absolutely satisfies the objectives of this study. The comparison of the impact of SVCs as the length of the transmission line varies showed under-reach and over reach tendencies for both zone 1 and zone 2.

The research revealed that as the length of the transmission line is increased the reliability of the fault locator when SVC is connected reduces as the distance relay tends to under-reach more for both zone 1

and zone 2. Although the under-reach phenomenon is much more pronounced on the zone 2 for medium transmission lines. For long transmission lines, the under-reach and over reach tendencies are more pronounced for zone 1 and zone 2 respectively.

The under-reach and over reach characteristics of the distance relay are clear indications that error margin in the fault location when SVC is connected for both zone 1 and zone 2.

5.1 Further research

Further research to develop an algorithm that can be implemented to reduce the errors introduced into the fault locator by the presence of SVCs on the Transmission Company of Nigeria (TCN) 132kV Power Grid Network.

Further study in the use of other types of FACTS devices is highly recommended using this same methodology.

Also, further study to simulate Zone 3 zone of protection is encouraged.

Declarations

Competing interests: The authors declare no competing interests.

References

1. B. M. a Amir Ghorbani a,⇑, Mojtaba Khederzadeh b, “Impact of SVC on the protection of transmission lines,” Elsevier Ltd, vol. 42, pp. 702–709, 2012.
2. IndustryArc, “Static VAR Compensator Market: By Type (Thyristor-Based SVC, & Magnetically Controlled Reactor-Based SVC) By End-Use Industry (Electric Utility, Renewable, Railway, Industrial, Oil & Gas, & Others), By Component & Geography - Forecast (2018–2023),” 2018. [Online]. Available: https://industryarc.com/Report/15449/static-var-compensator-market.html.
3. TCN, “About Tranmission COmpany of Nigeria,” *A breif history of TCN*, 2021. [Online]. Available: https://www.tcn.org.ng/page_history.php. [Accessed: 26-Dec-2021].
4. A. C. Mohamed ZELLAGUI, “IMPACT OF SVC DEVICES ON DISTANCE PROTECTION SETTING ZONES IN 400 kV TRANSMISSION LINE,” *U.P.B. Sci. Bull., Ser. C*, vol. 75, no. 2, pp. 249–262, 2013.
5. V. K. M. and R. Mehta, *Principles of Power System*, 4th Editio. Ram Nagar, New Delhi, India: S. Chand, 2012.
6. and D. T. V. Ngo Minh Khoa, Nguyen Huu Hieu2, “A Study of SVC’s Impact Simulation and Analysis for Distance Protection Relay on Transmission Lines,” Int. J. Electr. Comput. Eng., vol. 7, no. 4, pp. 1686–1695, 2017.
7. J. Lamture, “DEVELOPMENT OF DISTANCE RELAY IN MATLAB,” Int. J. Adv. Comput. Eng. Netw., vol. 3, no. 9, pp. 77–80, 2015.

8. P. G. and G. Sybille, “SVC (Detailed Model).” [Online]. Available: https://www.mathworks.com/help/physmod/sps/examples/svc-detailed-model.html. [Accessed: 08-Jul-2019].
9. A. N. Al-Husban, “An Eigenstructure Assignment for a Static Synchronous Compensator,” Am. J. Eng. Appl. Sci., vol. 2, no. 4, pp. 812–816, 2009.
10. T. T. N. Le Ngoc Giang*, Nguyen Thi Dieu Thuy, “Assessment study of STATCOM’s effectiveness in improving transient stability for power system,” TELKOMNIKA, vol. 11, no. 10, pp. 6095–6104, 2013.

Figures

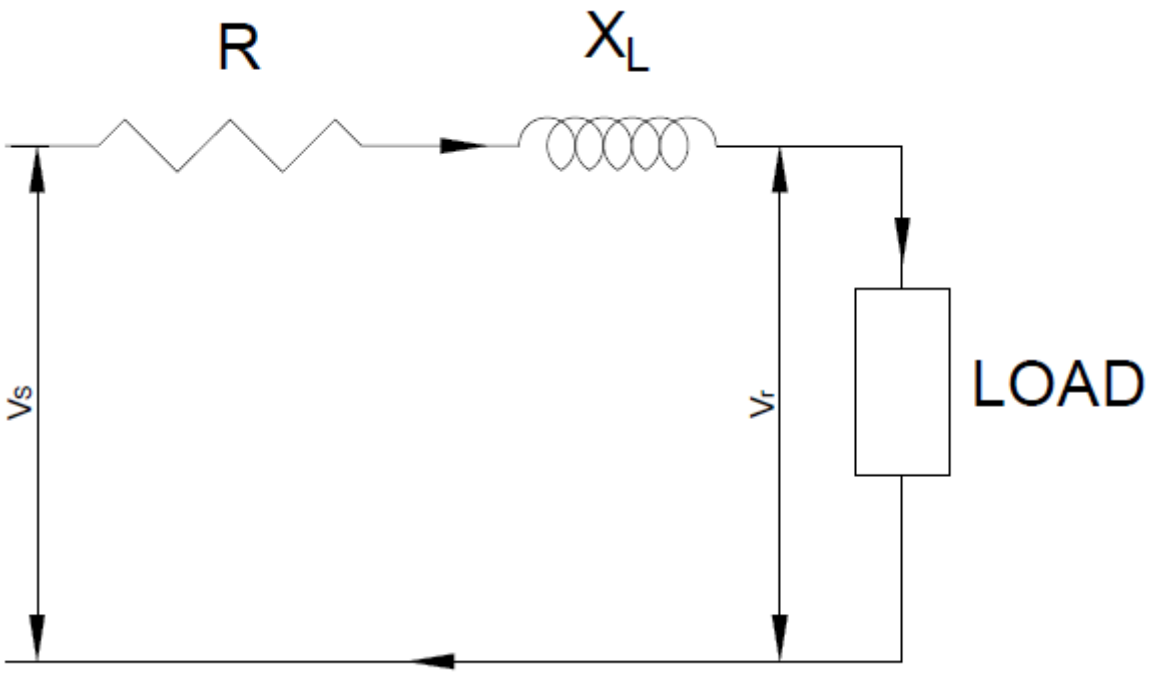

Figure 1

Diagram showing the equivalent circuit for a short transmission line [5].

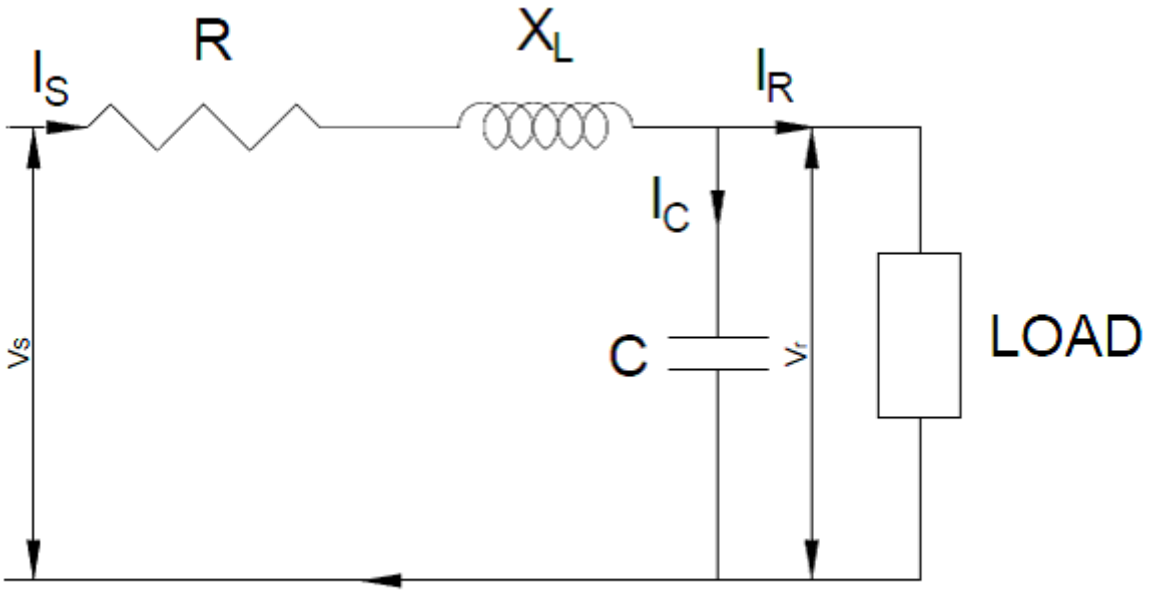

Figure 2

Diagram showing the equivalent circuit for an End condenser type of Medium transmission line modelling [5].

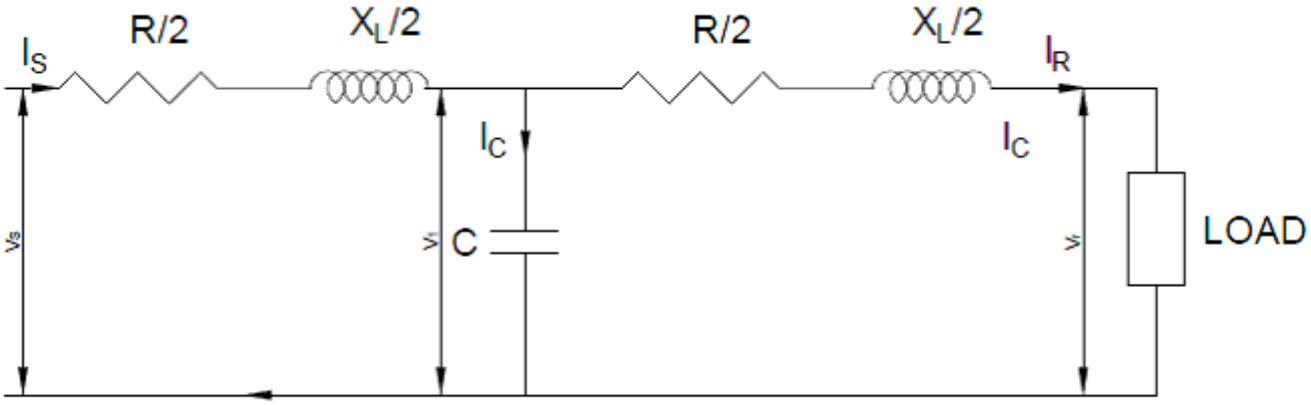

Figure 3

Diagram showing the equivalent circuit for a Nominal T type of Medium transmission line modelling [5].

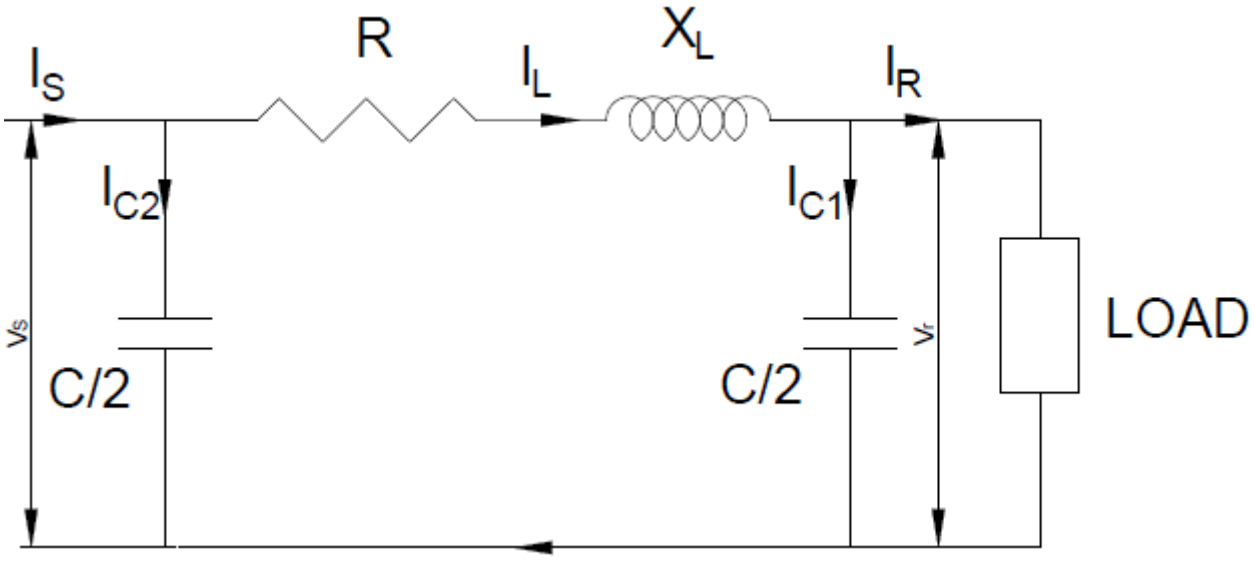

Figure 4

Diagram showing the equivalent circuit for a Nominal type of Medium transmission line modelling [5].

Figure 5

Diagram showing the equivalent circuit for a Long transmission line modelling [5]

Figure 6

Zones of protection of a transmission line

Figure 7

The Complete transmission line, distance relay and static var compensator model

Figure 8

The mho Circle graph

Figure 9

The Distance Relay Model

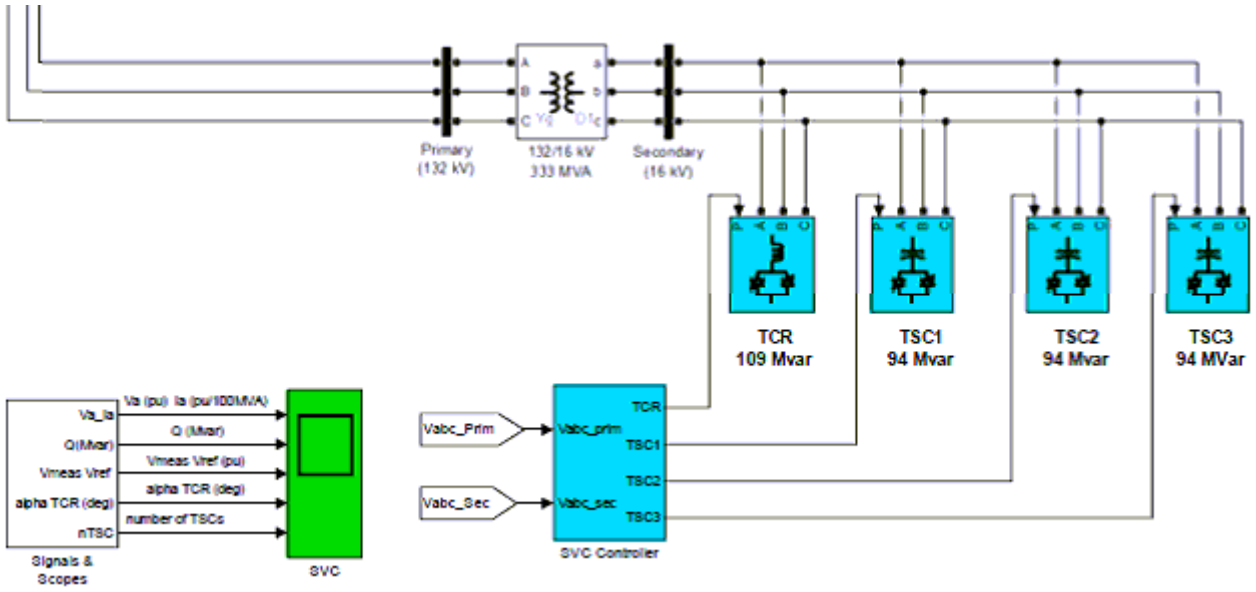

Figure 10

The Static Var Compensator (SVC) model

Figure 11

Resistance-Reactance (R-X) plot of a zone 1 for single Line-to-Earth fault with (a) with SVC (b) without SVC

Figure 12

Resistance-Reactance (R-X) plots of a zone 2 for single Line-to-Earth fault with (a) with SVC (b) without SVC

Figure 13

Resistance-Reactance (R-X) plot of a zone 1 for Three-Phase-to-Earth (L-L-L-E) fault with (a) with SVC (b) without SVC

Figure 14

Resistance-Reactance (R-X) plots of a zone 2 for Double Line-to-Earth (L-E) fault with (a) with SVC (b) without SVC

Figure 15

Resistance-Reactance (R-X) plot of a zone 1 for Line-to-Earth (L-E) fault with (a) with SVC (b) without SVC

Figure 16

Resistance-Reactance (R-X) plots of a zone 2 for Double Line-to-Earth (L-E) fault with (a) with SVC (b) without SVC

Figure 17

Distance relay response with and without the installation of SVC (a) 18.4km (short line) (b) 100km (medium line) (c) 226km